RESEARCH ARTICLE

Shotgun proteomics of extracellular matrix in late senescent human dermal fibroblasts reveals a down-regulated fibronectin-centered network

Kun Cho[1†], Kyeong Eun Yang[1†], Soo-Bin Nam[2,3], Song-I. Lee[4], Eui-Ju Yeo[4,5*] and Jong-Soon Choi[2,3*]

Abstract

Extracellular matrix (ECM) proteins play a pivotal role in cell growth and differentiation. To characterize aged ECM proteins, we compared the proteomes by shotgun method of young (passage #15) and late senescent (passage #40) human dermal fibroblasts (HDFs) using SDS-PAGE coupled with LC–MS/MS. The relative abundance of identified proteins was determined using mol% of individual proteins as a semi-quantitative index. Fifteen ECM proteins including apolipoprotein B (APOB) and high-temperature requirement factor 1 (HTRA1) were up-regulated, whereas 50 proteins including fibronectin 1 (FN1) and vitronectin (VTN) were down-regulated in late senescent HDFs. The identified ECM proteins combined with plasma membrane were queried to construct the protein–protein interaction network using Ingenuity Pathways Analysis, resulting in a distinct FN1-centered network. Of differentially abundant ECM proteins in shotgun proteomics, the protein levels of FN1, VTN, APOB, and HTRA1 were verified by immunoblot analysis. The results suggest that the aging process in HDFs might be finally involved in the impaired FN1 regulatory ECM network combined with altered interaction of neighboring proteins. Shotgun proteomics of highly aged HDFs provides insight for further studies of late senescence-related alterations in ECM proteins.

Keywords: Extracellular matrix, Human dermal fibroblasts, Late senescence, Shotgun proteomics, Protein network analysis

Introduction

Somatic cell population like human dermal fibroblasts (HDFs) undergoes a limited number of cell divisions before the dormant stage in which cell division stops. This phenomenon is called 'Hayflick limit', showing that a normal human fetal cell population can divide up to 60 times in certain cell culture condition (Hayflick and Moorhead 1961). However, it is generally accepted that the somatic cells are mortal except for stem cells. In contrast to dividing cells, senescent or late senescent (just before dormancy) cells display characteristic phenotypic alterations, such as G_0/G_1 cell cycle arrest (Demidenko and Blagosklonny 2008), higher senescence-associated β-galactosidase activity (Kurz et al. 2000), and hypo-responsiveness to growth factors (Kim et al. 2010). These changes contribute to the decline in cellular function accompanying the aging process.

Cellular senescence has been suggested to reduce the risk of neoplastic transformation by preventing cell proliferation. However, accumulating evidence presents that the senescent cells can have deleterious effects on tissue microenvironment, thereby contributing to late-life

---

[†]Kun Cho and Kyeong Eun Yang equally contributed in this study.

*Correspondence: euiju@gachon.ac.kr; jschoi@kbsi.re.kr

[2] Research Center for Materials Analysis, Korea Basic Science Institute, Daejeon 34133, Republic of Korea
[4] Department of Health Sciences and Technology, GAIHST, Gachon University, Incheon 21999, Republic of Korea
Full list of author information is available at the end of the article

cancers. Increased expression of vascular endothelial growth factor (VEGF) is a frequent characteristic of senescent human and mouse fibroblasts in culture (Coppe et al. 2006). Increased secretion of VEGF, much more in senescent fibroblasts than pre-senescent cells, stimulates tumor vascularization in aged mice facilitating age-associated cancer development. Other factors secreted from senescent fibroblasts are also known to alter senescent fibroblasts into pro-inflammatory cells (Coppe et al. 2010). Therefore, knowing what kinds of proteins are secreted by senescent somatic cells is very important for understanding and retarding the aging process.

Cells influence their own or neighboring microenvironment through the synthesis and secretion of a variety of extracellular matrix (ECM) components. Several ECM components are known to undergo changes during aging process (Lener et al. 2006) and in aging-related diseases, such as type II diabetes and Werner's syndrome (Labat-Robert and Robert 1988). The insoluble ECM factors secreted by senescent cells also contribute to cancer progression in aged organisms, suggesting the active role of ECM in determining cellular fate. As the human lifespan increases, interests and necessities in the wound healing of the elderly's skin are growing. In particular, the secreted ECM proteins provide a fundamental clue for skin regeneration. This study intends to attempt proteomic analysis of ECM of late senescent HDF cells. Although there were general reports related to ECM proteomics in HDFs (Yang et al. 2011; Won et al. 2012), a systematic ECM proteome analysis for late senescent skin cells has not been performed yet. Therefore, we performed comparative proteomic analysis of ECM proteins from young and late senescent HDFs to identify secreted proteins and to suggest their functional roles in aging process.

Materials and methods
Materials
DMEM, FBS, antibiotics (penicillin and streptomycin) were purchased from Gibco/BRL Life Technologies, Inc. (Carlsbad, CA). Monoclonal antibodies against fibronectin 1 (FN1) and vitronectin (VTN) were purchased from Chemicon (Bedford, MA), and monoclonal antibody against high-temperature requirement factor 1 (HTRA1) was from Abcam (Cambridge, MA). In addition, monoclonal antibodies against caveolin 1 (CAV1) and apolipoprotein B (APOB) were obtained from BD Biosciences Pharmingen (Mountain View, CA) and Santa Cruz Biotechnology, Inc. (Santa Cruz, CA), respectively. HRP-conjugated anti-rabbit and anti-mouse secondary antibodies were obtained from Vector Laboratories (Burlingame, CA). The protein assay kit was purchased

from Bio-Rad Laboratories (Hercules, CA), and the ECL system was purchased from GE Healthcare (Buckinghamshire, UK).

Cell culture and preparation of ECM
Neonatal HDFs were isolated from neonates as described previously (Tomela et al. 2021). Briefly, cells were obtained from Seoul National University (SNU) and cultured at 37 °C, 5% CO_2 in DMEM supplemented with 10% FBS, 100 units/ml penicillin, and 100 µg/ml streptomycin. Cells with passage #15, #30 and #40 were considered young, early senescent, and late senescent (or near quiescent) state, respectively. ECM proteins were prepared from cultured population doublings (PD) 15 and PD 40 HDFs as described previously (Yeo et al. 2000). The matrices after trypsinized HDFs were scraped out and resuspended in 10 mM Tris–HCl buffer (pH 7.2) containing 1% Triton X-100, 10% glycerol, 5% sodium dodecyl sulfate (SDS), 100 mM DTT, and 1% protease inhibitor cocktail. Protein concentrations were estimated using the BCA™ protein assay kit. The filtrates were passed through the 1 kDa cut-off Centricon filter and vacuum dried samples were stored at -70 °C prior to LC–MS analysis.

Senescent-associated β-galactosidase assay
Senescence indices using senescence-associated β-galactosidase (SA-β-Gal) in passage #15, #30, and #40 HDFs were detected by Senescence Cells Histochemical Staining kit (Sigma-Aldrich, Seoul, Korea). SA-β-Gal analysis was performed as described previously (Pflieger et al. 2006).

Proteomic analysis of ECM protein extracts
Proteins (50 µg) were loaded on 3-8% Tris–acetate gel. After running on SDS-PAGE, gels were fixed in 30% ethanol/7.5% acetic acid for 2 h followed by staining with Coomassie Brilliant Blue R250. Each gel lane was cut into 12 pieces and each piece was transferred to a new Eppendorf tube. The sliced gel piece was washed with 10 mM ammonium bicarbonate (ABC) and 50% acetonitrile and incubated in tryptic digestion buffer containing 50 mM ABC, 5 mM $CaCl_2$, and 1 mg/ml trypsin at 37 °C for 16 h. Peptides were recovered by two cycles of extraction with 50 mM ABC and 100% acetonitrile. The lyophilized peptide extracts were dissolved in 0.1% formic acid and analyzed by LC–MS/MS as described previously (Kim et al. 2005). Eluted peptides were applied to a 7-Tesla Fourier Transform-Ion Cyclotron Resonance (FT-ICR) MS (Thermo Fisher, San Jose, CA). For LC separation, a microcapillary column (75 µm × 150 mm) packed with C_{18} silica resin was used. The mobile phases, A and B, were composed of 0 and 100% acetonitrile, respectively,

Cho *et al. Journal of Analytical Science and Technology*   (2022) 13:20

Page 3 of 10

each containing formic acid (0.1%). MS-derived peptides were searched against the human database of International Protein Index (http://www.ebi.ac.uk/IPI) using the Mascot program version 2.2 (http://www.matrixscience.com, Matrixscience, London, UK). Peptide MS/MS assignments were filtered as the criteria: peptide tolerance of parental ion was set at 50 ppm and MS/MS tolerance at 0.8 Da. Carbamidomethylation of cysteine ($+57$ Da) and oxidation of methionine ($+16$ Da) were chosen as variable modifications. In addition, one missed cleavage of trypsin was allowed for peptide identification. MS and MS/MS spectra with Mascot scores higher than the probability ($P<0.01$ and $P<0.05$, respectively) were considered valid. As an indication of identification certainty, the false discovery rate for peptide and protein matches above identity threshold was calculated by Peptide Validator at 1.0%. The peptide score is $-10 \times \text{Log}\,(P)$, where P is the probability that anobserved match is a random event. Individual peptide scores were considered as identity or extensive homology ($P<0.01$).

For statistical evaluation, a two-sided *t*-test was used. The p value was corrected using false discovery rate (FDR) based multiple hypothesis testing. Both t-test and FDR based multiple hypothesis testing were carried out with the default settings of the Perseus statistics software. All data were normalized using a linear regression analysis.

Protein–protein interaction analysis

To infer the biological functions of plasma membrane and ECM proteins through their interaction network, protein network analysis was performed using Ingenuity Pathways Analysis (IPA, http://www.ingenuity.com). IPA provides the identified protein interaction network on the basis of a regularly updated "Ingenuity Pathways Knowledge-base." Ingenuity Pathways Knowledge-base is an updatable database containing millions of individual protein–protein relationships retrieved from literature (Rather et al. 2022). Network generation is optimized for the inclusion of many proteins as possible from the input expression profile and aimed at the production of highly connected networks.

Immunoblot analysis

ECM protein expression levels were confirmed by immunoblot analysis as described previously (Kwon et al. 2010). ECM protein lysates were prepared in a lysis buffer containing 50 mM Tris–HCl (pH 7.5), 150 mM NaCl, 2 mM EDTA, 1 mM EGTA, 1 mM Na_3VO_4, 10 mM NaF, 1 mM DTT, 1 mM PMSF, 25 μg/ml leupeptin, 25 μg/ml aprotinin, 5 mM benzamidine, and 1% Ingepal CA630. Protein concentrations were determined using the Bio-Rad protein assay kit according to the manufacturer's protocol. Equal amounts of ECM proteins (45 μg) isolated from passage #15 and #40 HDFs were resolved by SDS-PAGE and transferred onto Immobilon PVDF membranes. Blots were blocked with a solution containing 5% nonfat dried milk or 5% BSA and 0.1% Tween 20 and incubated with primary antibody in blocking solution overnight. And the blots were washed and further probed with HRP-conjugated anti-rabbit IgG (1: 5,000). The immune complexes were visualized using the ECL detection system according to the manufacturer's protocol. Antibodies against FN1, VTN, HTRA1, CAV1, and APOB were used for immunoblot analysis.

Statistical analysis

Significant differences between the mean values of expressed protein levels from passage #15 and #40 HDFs were determined by Student *t*-test with Graph-Pad Prism (GraphPad, San Diego, CA). Data were presented as means ± standard deviation from triplicate performances. Statistical *P* values less than 0.05 were considered as significant.

Results and discussion

In the present study, we examined the senescence states of passage #15, #30, and #40 HDFs using SA-β-Gal staining. According to previous reports, SA-β-Gal positive cell% in young HDFs showed less than 5% in young cells to ~80% in senescent cells (Jang et al. 2019; Yang et al. 2020). Likewise, SA-β-Gal positive cell% of passage #15 was 14%, while those cell% of passage #30 and #40 HDFs were 46% ($P<0.01$) and 83% ($P<0.001$) stained, respectively (Fig. 1). The passage number that reaches senescence depends on the origin of the HDF cells. ATCC-derived HDFs have a passage number of 17 to reach senescence, which is shorter than the passage number 35 to reach senescence in SNU-derived cells (Yang et al. 2020; Jang et al. 2020). In our study, we defined passage #30 and #40 cells as early and late senescent state on the basis of SA-β-Gal staining.

Next, we characterized the ECM proteins of young and late senescent HDFs to identify late senescence-related proteins (Additional file 1: Table S1, Additional file 2: Table S2, Additional file 3: Table S3 and Additional file 4: Table S4). Protein separation and analysis were accomplished by SDS-PAGE and in-gel tryptic digestion, followed by high-resolution 7-Tesla FT-ICR. The use of these techniques is known as shotgun proteomics as described previously (Cargile et al. 2004). ECM proteins from young and late senescent HDFs were resolved by SDS-PAGE and each lane was cut into 12 gel pieces for subsequent in-gel tryptic digestion (data not shown). The trypsin-digested peptides were separated by reverse-phase LC and identified by 7-Tesla FT-ICR MS analysis.

Cho *et al. Journal of Analytical Science and Technology*   (2022) 13:20

Page 4 of 10
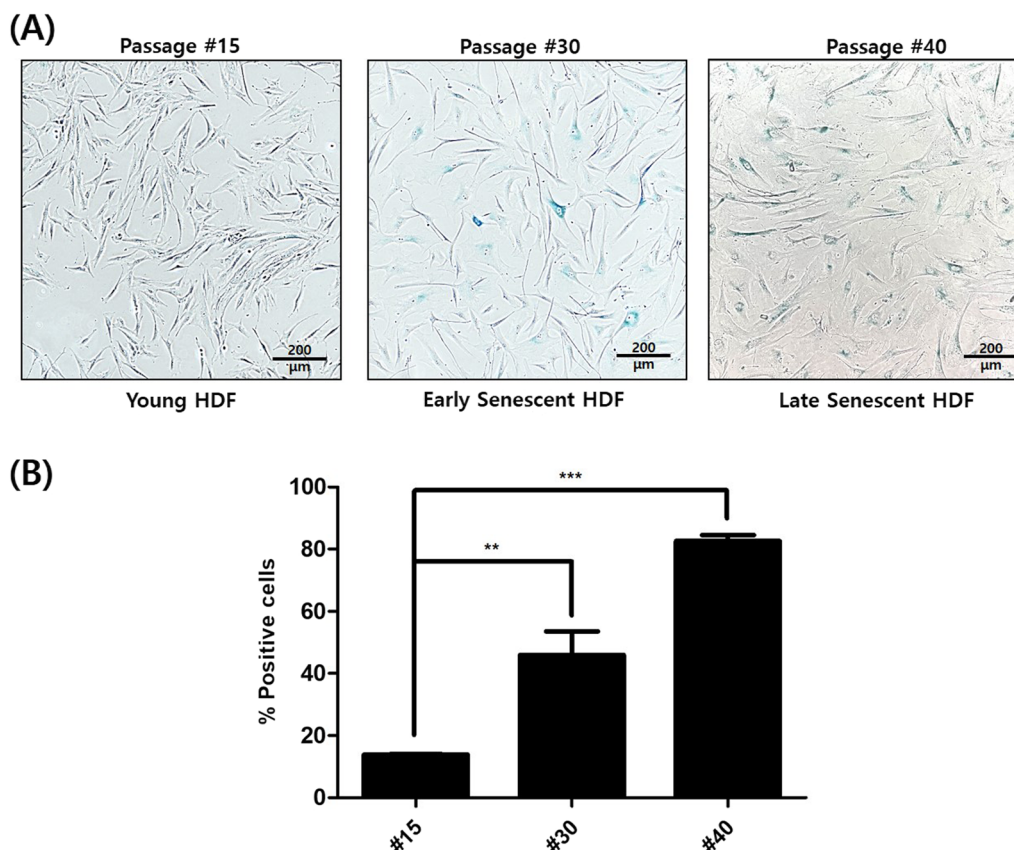
Fig. 1 SA-β-Gal staining of HDFs. **A** Light microscopic images of young HDFs (passage #15) and late senescent HDFs (passage #40) are presented. **B** Quantification of SA-β-Gal-positive cells% of HDFs. Data represent the mean ± standard deviation of triplicate experiments. **Statistical significance $P < 0.001$

Shotgun proteomic analysis revealed that MS/MS spectra from young (111,817 spectra) and late senescent HDFs (99,255 spectra) resulted in 3458 and 3287 peptides, respectively. Using Mascot search against human IPI dataset, a total of 189 proteins were finally identified, which the proteins were categorized on the basis of intracellular localization of IPA annotation: cytoplasm (40%), ECM (35%), nucleus (2%), plasma membrane (10%), and unknown (14%). Semi-quantitative analysis of ECM proteins was performed to calculate the mol% of individual proteins derived from the exponentially modified protein abundance index (Ishihama et al. 2005). Fold changes in mol% were also calculated to compare the relative abundance of ECM proteins between young and late senescent HDFs, as listed in Table 1. As shown in Table 1, 50 ECM proteins were differentially expressed: 15 ECM proteins were up-regulated and 50 ECM proteins were down-regulated in late senescent HDFs compared to young HDFs.

In order to explore hub proteins in the extracellular region of late senescent HDFs, a total of 83 proteins expressed in the plasma membrane and ECM were queried to IPA, resulting in a distinct network interconnected with 59 proteins (Fig. 2). IPA is a web-based software that facilitates the network of protein–protein interactions in silico based on the collated interactions and associations reported in the literature (Deighton et al. 2010). As shown in IPA analysis, FN1 was at the center of the protein network. FN1, a major ECM glycoprotein, binds to integrin and other ECM proteins either directly or indirectly and is involved in various biological functions, such as adhesion, growth, migration, and differentiation (Ksiazek et al. 2009). FN1-associated proteins included VTN, CAV1, APOB, and HTRA1 (Fig. 2). FN1 was exclusively observed in young HDFs, whereas APOB and HTRA1 were mainly present in late senescent HDFs (Table 1). The relative abundance of VTN and CAV1 was not significantly different between young and late senescent HDFs. However, VTN and CAV1 are directly linked to FN1 hub protein. Thus, biochemical validations of FN1, APOB, HTRA1 including VTN and CAV1 were conducted.

Cho *et al. Journal of Analytical Science and Technology* (2022) 13:20

Page 5 of 10

Table 1 List of differentially abundant ECM proteins between passage #15 and #40 HDFs

IPI accession no.[a]	Gene symbol[b]	Protein name	mol%[c]		Fold change[d]
			#40	#15	
Increased ECM proteins in late senescent HDFs					
IPI00914848	SERPINE2	Isoform 2 of Glia-derived nexin	0.24		#40
IPI00306543	GDF15	Growth/differentiation factor 15	0.20		#40
IPI00026941	PRSS23	Serine protease 23	0.16		#40
IPI00179185	CPZ	Isoform 2 of Carboxypeptidase Z	0.10		#40
IPI00022229	APOB	Apolipoprotein B-100	0.02		#40
IPI00554711	JUP	Junction plakoglobin	0.08		#40
IPI00013933	DSP	Isoform DPI of Desmoplakin	0.03		#40
IPI00003176	HTRA1	Serine protease HTRA1	1.15	0.25	4.565
IPI00022937	F5	252 kDa protein	0.07	0.03	2.213
IPI00025753	DSG1	Desmoglein-1	0.15	0.08	1.881
IPI00022420	RBP4	Retinol-binding protein 4	0.52	0.28	1.814
IPI00027547	DCD	Dermcidin	2.04	1.16	1.762
IPI00218247	TIMP3	Metalloproteinase inhibitor 3	0.70	0.43	1.610
IPI00218918	ANXA1	Annexin A1	0.39	0.25	1.556
IPI00300725	KRT6A	Keratin, type II cytoskeletal 6A	1.70	1.15	1.478
Decreased ECM proteins in late senescent HDFs					
IPI00873923	TGFBI	Transforming growth factor, beta-induced, 68 kDa, isoform CRA_a		9.98	#15
IPI00009890	SERPINE2	Isoform 1 of Glia-derived nexin		0.50	#15
IPI00218732	PON1	Serum paraoxonase/arylesterase 1		0.34	#15
IPI00221224	ANPEP	Aminopeptidase N		0.31	#15
IPI00029928	ELN	Elastin		0.24	#15
IPI00789324	JUP	cDNA FLJ60424, highly similar to Junction plakoglobin		0.21	#15
IPI00219682	STOM	Erythrocyte band 7 integral membrane protein		0.20	#15
IPI00009456	NT5E	5~-nucleotidase		0.15	#15
IPI00027482	SERPINA6	Corticosteroid-binding globulin		0.13	#15
IPI00328609	SERPINA4	Kallistatin		0.13	#15
IPI00550731	IGKC	Putative uncharacterized protein		0.12	#15
IPI00022895	A1BG	Alpha-1B-glycoprotein		0.11	#15
IPI00479116	CPN2	Carboxypeptidase N subunit 2		0.10	#15
IPI00022395	C9	Complement component C9		0.09	#15
IPI00018305	IGFBP3	Insulin-like growth factor-binding protein 3		0.09	#15
IPI00294395	C8B	Complement component C8 beta chain		0.09	#15
IPI00879709	C6	Complement component 6 precursor		0.06	#15
IPI00022371	HRG	Histidine-rich glycoprotein		0.05	#15
IPI00025864	BCHE	Cholinesterase precursor		0.04	#15
IPI00294004	PROS1	Vitamin K-dependent protein S		0.04	#15
IPI00339223	FN1	Isoform 3 of Fibronectin		0.03	#15
IPI00017640	SLIT3	Isoform 1 of Slit homolog 3 protein		0.03	#15
IPI00017601	CP	Ceruloplasmin		0.02	#15
IPI00217182	DSP	Isoform DPII of Desmoplakin		0.02	#15
IPI00031008	TNC	Isoform 1 of Tenascin		0.02	#15
IPI00022200	COL6A3	Isoform 1 of Collagen alpha-3(VI) chain		0.02	#15
IPI00022488	HPX	Hemopexin	0.13	0.69	− 5.241
IPI00555812	GC	Isoform 1 of Vitamin D-binding protein	0.06	0.24	− 4.002
IPI0292530	ITIH1	Inter-alpha-trypsin inhibitor heavy chain H1	0.10	0.38	− 3.943
IPI00026314	GSN	Isoform 1 of Gelsolin	0.12	0.47	− 3.808

Cho *et al. Journal of Analytical Science and Technology*   (2022) 13:20

Page 6 of 10

Table 1 (continued)

IPI accession no.[a]	Gene symbol[b]	Protein name	mol%[c]		Fold change[d]
			#40	#15	
IPI00007960	POSTN	Isoform 1 of Periostin	0.07	0.24	− 3.502
IPI00022431	AHSG	cDNA FLJ55606, highly similar to Alpha-2-HS-glycoprotein	0.15	0.47	− 3.136
IPI00022426	AMBP	Protein AMBP	0.09	0.25	− 2.892
IPI00011252	C8A	Complement component C8 alpha chain	0.05	0.14	− 2.711
IPI00021841	APOA1	Apolipoprotein A-I	0.37	0.99	− 2.690
IPI00029739	CFH	Isoform 1 of Complement factor H	0.04	0.11	− 2.530
IPI00550991	SERPINA3	cDNA FLJ35730 fis, clone TESTI2003131, highly similar to ALPHA-1-ANTICHYMOTRYPSIN	0.38	0.94	− 2.501
IPI00305461	ITIH2	Inter-alpha-trypsin inhibitor heavy chain H2	0.27	0.67	− 2.478
IPI00032291	C5	Complement C5	0.03	0.08	− 2.259
IPI00032179	SERPINC1	Antithrombin-III	0.36	0.77	− 2.160
IPI00021857	APOC3	Apolipoprotein C-III	0.32	0.69	− 2.125
IPI00071509	PKP1	Isoform 2 of Plakophilin-1	0.03	0.07	− 2.033
IPI00021842	APOE	Apolipoprotein E	0.09	0.17	− 1.988
IPI00219365	MSN	Moesin	0.04	0.09	− 1.988
IPI00291866	SERPING1	Plasma protease C1 inhibitor	0.12	0.24	− 1.936
IPI00292946	SERPINA7	Thyroxine-binding globulin	0.07	0.13	− 1.920
IPI00478003	A2M	Alpha-2-macroglobulin	0.10	0.20	− 1.883
IPI00163207	PGLYRP2	Isoform 1 of N-acetylmuramoyl-L-alanine amidase	0.05	0.09	− 1.807
IPI00292950	SERPIND1	Serpin peptidase inhibitor, clade D (Heparin cofactor), member 1	0.17	0.28	− 1.581
IPI00296099	THBS1	Thrombospondin-1	0.08	0.12	− 1.506

[a] Accession numbers of identified proteins were from the International Protein Index (IPI) Human database

[b] HUGO gene symbols of mapped proteins were taken from the Ingenuity Pathways Analysis software

[c] Mol% of identified proteins was calculated using the exponentially modified protein abundance index (emPAI) value based on the number of identified peptides
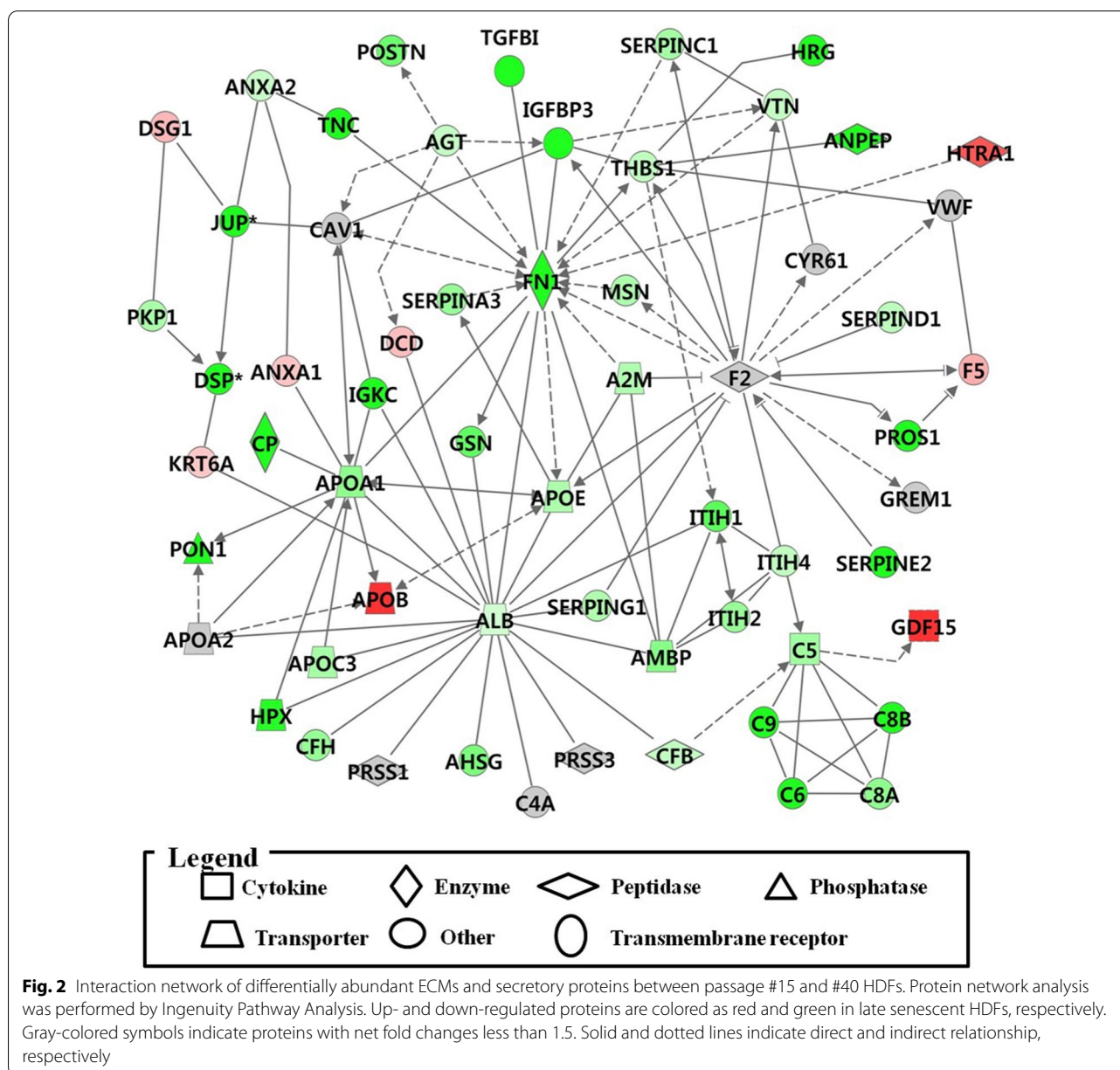
[d] Fold change was calculated by dividing the protein's mol% of PD 40 HDFs by protein's mol% of passage #15 HDFs. If this number was less than 1, a negative sign was added to the reciprocal number. If the original fold change was calculated as 0.75, the negative sign of the calculated fold change was added to the reciprocal number, resulting in − 1.33. "passage #40" or "passage #15" indicates the exclusively identified protein in each group

Additionally, the possible roles of target ECM proteins directed connected to FN1 were described hereafter.

The protein levels of VTN and CAV1 were significantly altered in late senescent HDFs. The immunoblot analysis revealed that VTN was slightly reduced but CAV1 dramatically increased in late senescent ECM (Fig. 3). The differences between passage #15 and #40 HDFs were detected significantly at $P < 0.001$. Interestingly, FN1 is known to be an age-related marker protein due to its increased protein and mRNA levels in senescent cells (Matos et al. 2012). Contrast to the previous report, the expression levels of FN1 in late senescent HDFs were observed down-regulated. We suggest that the cellular FN1 is involved in a fibrillary network forming detergent-insoluble fibrils and the fibrillary fibronectin has been reduced or absent on the surface of late-passage cells as cited previously (Wierzbicka-Patynowski et al. 2004; Wang et al. 2022). Furthermore, cellular aging is associated with the proteolytic degradation of ECM proteins (Labat-Robert 2003). Increased elastase-type activity,

gelatinase, Ca^{2+}-dependent fibronectinase, matrix metalloproteinases (MMPs), and cathepsin G have been implicated in FN fragmentation in the ECM (Hibbert et al. 2019). Therefore, proteolysis of FN may be responsible for the reduction of FN in ECM of senescent fibroblasts.

In the present study, VTN was slightly down-regulated in the matrix of late senescent HDFs (Table 1 and Fig. 3). Similar to FN1, cellular aging-associated proteolysis of VTN may be responsible for decreased VTN in late senescent ECM. VTN plays a role in several processes, such as hemostasis, vascular remodeling, phagocytosis, tumor growth and metastasis, wound healing, and viral infection (Budatha et al. 2021). Indeed, the binding of urokinase plasminogen activator (uPA) to uPA receptor (uPAR) induces the activation of plasminogen to plasmin, which favors proteolysis of ECM proteins and converts VTN into defined fragments (Kost et al. 1996). VTN is considered a promising rejuvenation marker due to its anti-aging effect. Since CAV1 is overexpressed in dermal and subdermal cells during chronological and

Cho *et al. Journal of Analytical Science and Technology* (2022) 13:20

Page 7 of 10

Fig. 2 Interaction network of differentially abundant ECMs and secretory proteins between passage #15 and #40 HDFs. Protein network analysis was performed by Ingenuity Pathway Analysis. Up- and down-regulated proteins are colored as red and green in late senescent HDFs, respectively. Gray-colored symbols indicate proteins with net fold changes less than 1.5. Solid and dotted lines indicate direct and indirect relationship, respectively

UV-induced aging, CAV1 has been suggested to play a key role in cellular senescence and skin aging (Jang et al. 2019). CAV1 directly interacts with receptors and signaling molecules, such as transforming growth factor beta (TGF-β), toll-like and glucocorticoid receptors, MMPs, and heat shock proteins (Kruglikov et al. 2019). Since CAV1 is highly expressed in different hyper-proliferative and inflammatory skin diseases, the regulation of CAV1 is considered a treatment strategy in dermatology (Kruglikov and Scherer 2019). Although CAV1 has been known to be age-related protein marker, we did not detect CAV1 by shotgun proteomics in the present study. Presumably,

it is due to the limitation of protein sample preparation. However, the immunoblot analysis of passage #15 and #40 HDFs revealed to be significantly increased in late senescent HDFs (Fig. 3). These results are consistent with those of previous reports (Kim et al. 2010; Jang et al. 2019).

APOB, the main protein found in low-density lipoprotein (LDL), selectively interacts with the constituents of ECM, such as collagen, proteoglycans, and glycosaminoglycans (Hevonoja et al. 2000). The present study showed that five apolipoprotein isoforms, APOA1, APOA2, APOB, APOC3, and APOE, were directly or
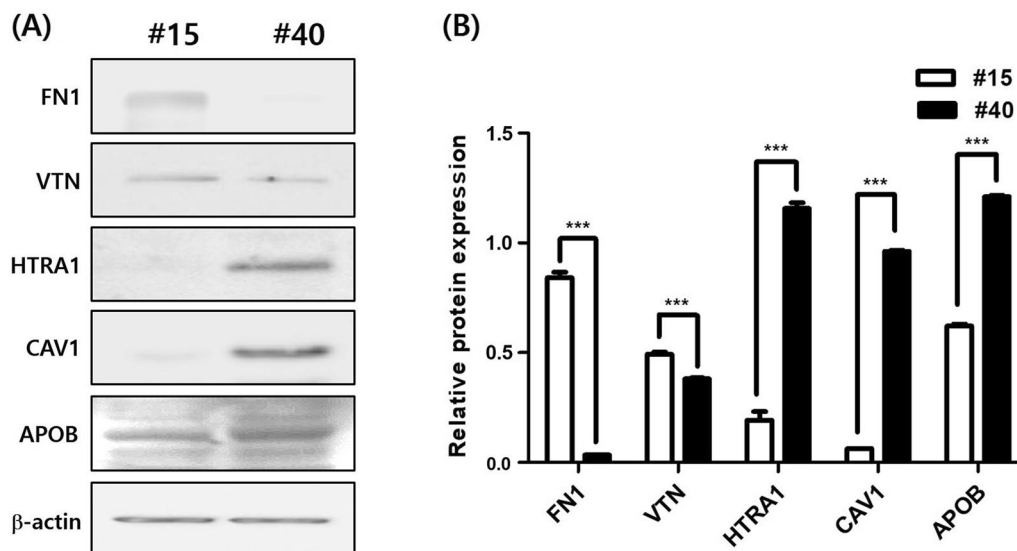
Fig. 3 Immunoblot analysis of ECM proteins. **A** Images of expressed ECM proteins in passage #15 and #40 HDFs. Equal amount of ECM proteins (45 μg) from sub-confluent young and late senescent fibroblasts were used for immunoblot analysis with antibodies against FN1, VTN, HTRA1, CAV1, and APOB. **B** Quantification of protein expression levels. Relative expression levels of ECM proteins were quantified with β-actin as a house-keeping protein. Quantification was performed using Image J program. ***Statistical significance $P < 0.001$

indirectly linked to FN1 subnet hub protein (Fig. 2). Among them, APOA1, APOC3, and APOE were mainly present in young HDFs, whereas APOB was exclusively present in late senescent HDFs (Table 1). The protein levels of APOB were significantly higher in late senescent HDFs than in young cells (Fig. 3). These results are consistent with the previous report demonstrating that the accumulation of APOB was associated with aging in retinal pigment epithelium (Curcio et al. 2010). HTRA1 is a secretory protein that is indirectly linked to FN1 and functions as a heat shock serine protease activated by external stress (Yang et al. 2006). HTRA1 has been validated as an aging marker of age-related macular degeneration (Gu et al. 2009). Herein, the expression levels of HTRA1 were approximately 4.6-fold higher in the ECM of late senescent fibroblasts than in young cells (Table 1). As expected, the protein levels of HTRA1 were significantly higher in late senescent HDFs than in young cells (Fig. 3). Interestingly, HTRA1 is known to inhibit the signaling of TGF-β family proteins (Oka et al. 2004). Recently, HTRA1 has been associated with frailty status in older adults (Lorenzi et al. 2016). Since chronic inflammation may be involved in the pathogenesis of frailty, HTRA1, as an inhibitor of anti-inflammatory cytokine TGF-β, seems to be a causative factor for frailty in older adults. HTRA1 has also been implicated in several age-associated diseases, such as Alzheimer's disease (Grau et al. 2005).

Besides the proteins mentioned above, it is notable to describe several proteins expressed exclusively in young or late senescent state of HDFs. The expression levels of GDF15 belonged to proteins expressed exclusively in late senescent state are increased in UV-irradiated senescent fibroblasts (Kim et al. 2020). The cytoskeletal protein, desmosome (JUP), belonged to exclusive expressions in late senescent HDFs, were reduced in aged skin tissue (Oender et al. 2008). Next, the proteins expressed exclusively in early stage contain PON1, Eln, IGFBP-3, and COL6A1. Paraoxonase 1 (PON1)-targeted human dermal microvascular endothelial cells are turned into cellular senescence (Lee et al. 2012). Likewise, the elastin (Eln) is associated with a loss in aging process (Lasio and Kozel 2018) and the function of IGFBP-3 is considered important at early stage of aging (Song et al. 2018). Mutation of collagen VI containing COL6A1 may lead to skin abnormality (Lettmann et al. 2014).

Conclusions

Shotgun proteomics combined with IPA-based protein network analysis presented that FN1-centered ECM and secretory proteins were differentially expressed in young and late senescent HDFs. The finally identified proteins including FN1, VTN, APOB, and HTRA1 were significantly altered in late senescent HDFs compared to young cells. Comparative proteomic approach using late senescent HDFs clearly revealed potential aging-related

Cho *et al. Journal of Analytical Science and Technology* (2022) 13:20

Page 9 of 10

markers. The applications to these ECM proteins might give some clues to cure the aged human skin.

Supplementary Information

The online version contains supplementary material available at https://doi.org/10.1186/s40543-022-00329-2.

Additional file 1: Table S1.

Additional file 2: Table S2.

Additional file 3: Table S3.

Additional file 4: Table S4.

Author contributions

Conceptualization and data curation, JSC and KC; methodology, KC; validation, KC and KEY; formal analysis, KC, and SBN; investigation, JSC and EJY; writing-original draft preparation, KC; writing-review and editing, JSC and SIL; supervision, JSC and KC. All authors read and approved the final manuscript.

Availability of data and materials

All relevant data are within the paper and in the supplementary file.

Declarations

Competing interests

The authors declare no conflict of interest. The authors also stated that "The funders had no role in the design of the study; in the collection, analyses, or interpretation of data; in the writing of the manuscript, or in the decision to publish the results".

Author details

[1]Bio-Chemical Analysis Team, Center for Research Equipment, Korea Basic Science Institute, Daejeon 34133, Republic of Korea. [2]Research Center for Materials Analysis, Korea Basic Science Institute, Daejeon 34133, Republic of Korea. [3]Graduate School of Analytical Science and Technology, Chungnam National University, Daejeon 34134, Republic of Korea. [4]Department of Health Sciences and Technology, GAIHST, Gachon University, Incheon 21999, Republic of Korea. [5]Department of Biochemistry, College of Medicine, Gachon University, Incheon 21999, Republic of Korea.

References

Budatha M, Zhang J, Schwartz MA. Fibronectin-mediated inflammatory signaling through integrin α5 in vascular remodeling. J Am Heart Assoc. 2021;10: e021160.

Cargile BJ, Bundy JL, Grunden AM, Stephenson JL Jr. Synthesis/degradation ratio mass spectrometry for measuring relative dynamic protein turnover. Anal Chem. 2004;76:86–97.

Coppe JP, Kauser K, Campisi J, Beausejour CM. Secretion of vascular endothelial growth factor by primary human fibroblasts at senescence. J Biol Chem. 2006;281:29568–74.

Coppe JP, Desprez PY, Krtolica A, Campisi J. The senescence-associated secretory phenotype: the dark side of tumor suppression. Ann Rev Pathol. 2010;5:99–118.

Curcio CA, Johnson M, Huang JD, Rudolf M. Apolipoprotein B-containing lipoproteins in retinal aging and age-related macular degeneration. J Lipid Res. 2010;51:451–67.

Deighton RF, Kerr LE, Short DM, Allerhand M, Whittle IR, McCulloch J. Network generation enhances interpretation of proteomic data from induced apoptosis. Proteomics. 2010;10:1307–15.

Demidenko ZN, Blagosklonny MV. Growth stimulation leads to cellular senescence when the cell cycle is blocked. Cell Cycle. 2008;7:3355–61.

Grau S, Baldi A, Bussani R, Tian X, Stefanescu R, Przybylski M, Richards P, Jones SA, Shridhar V, Clausen T, Ehrmann M. Implications of the serine protease HtrA1 in amyloid precursor protein processing. Proc Natl Acad Sci USA. 2005;102:6021–6.

Gu J, Pauer GJT, Yue X, Narendra U, Sturgill GM, Bena J, Gu X, Peachey NS, Salomon RG, Hagstrom SA, Crabb JW, Clinical Genomic and Proteomic AMD Study Group. Assessing susceptibility to age-related macular degeneration with proteomic and genomic biomarkers. Mol Cell Proteomics. 2009;8:1338–49.

Hayflick L, Moorhead PS. The serial cultivation of human diploid cell strains. Exp Cell Res. 1961;25:585–621.

Hevonoja T, Pentikainen MO, Hyvonen MT, Kovanen PT, Ala-Korpela M. Structure of low density lipoprotein (LDL) particles: basis for understanding molecular changes in modified LDL. Biochim Biophys Acta. 2000;1488:189–210.

Hibbert SA, Watson REB, Griffiths CEM, Gibbs NK, Sherratt MJ. Selective proteolysis by matrix metalloproteinases of photo-oxidised dermal extracellular matrix proteins. Cell Signal. 2019;54:191–9.

Ishihama Y, Oda Y, Tabata T, Sato T, Nagasu T, Rappsilber J, Mann M. Exponentially modified protein abundance index (emPAI) for estimation of absolute protein amount in proteomics by the number of sequenced peptides per protein. Mol Cell Proteomics. 2005;4:1265–72.

Jang H-J, Yang KE, Oh WK, Lee S-I, Hwang I-H, Ban K-T, Yoo H-S, Choi J-S, Yeo E-J, Jang I-S. Nectandrin B-mediated activation of the AMPK pathway prevents cellular senescence in human diploid fibroblasts by reducing intracellular ROS levels. Aging. 2019;11(11):3731–49.

Jang I-S, Jo E, Park SJ, Baek SJ, Hwang I-H, Kang HM, Lee J-H, Kwon J, Son J, Kwon HJ, Choi J-S. Proteomic analyses reveal that finsenoside Rg3(S) partially reverses cellular senescence in human dermal fibroblasts by inducing peroxiredoxin. J Ginseng Res. 2020;44:50–7.

Kim JY, Lee JH, Park GW, Cho K, Kwon KH, Park YM, Cho SY, Paik Y-K, Yoo JS. Utility of electrophoretically derived protein mass estimates as additional constraints in proteome analysis of human serum based on MS/MS analysis. Proteomics. 2005;5:3376–85.

Kim SY, Ryu SJ, Ahn HJ, Choi HR, Kang HT, Park SC. Senescence-related functional nuclear barrier by down-regulation of nucleo-cytoplasmic trafficking gene expression. Biochem Biophys Res Comm. 2010;391:28–32.

Kim Y, Kang B, Kim JC, Park TJ, Kang HY. Senescent fibroblast-derived GDF15 induces skin prgmentation. J Investig Dermatol. 2020;140:2478–86.

Kost C, Benner K, Stockmann A, Linder D, Preissner KT. Limited plasmin proteolysis of vitronectin. Characterization of the adhesion protein as morpho-regulatory and angiostatin-binding factor. Eur J Biochem. 1996;236:682–8.

Kruglikov IL, Scherer PE. Caveolin as a universal target in dermatology. Int J Mol Sci. 2019;21:80.

Kruglikov IL, Zhang Z, Scherer PE. Caveolin-1 in skin aging—from innocent bystander to major contributor. Ageing Res Rev. 2019;55: 100959.

Ksiazek K, Mikula-Pietrasik J, Korybalska K, Dworacki G, Jörres A, Witowski J. Senescent peritoneal mesothelial cells promote ovarian cancer cell adhesion: the role of oxidative stress-induced fibronectin. Am J Pathol. 2009;174:1230–40.

Kurz DJ, Decary S, Hong Y, Erusalimsky JD. Senescence-associated (beta)-galactosidase reflects an increase in lysosomal mass during replicative ageing of human endothelial cells. J Cell Sci. 2000;113(Pt 20):3613–22.

Kwon HJ, Rhim JH, Jang I-S, Kim G-E, Park SC, Yeo E-J. Activation of AMP-activated protein kinase stimulates the nuclear localization of glyceraldehyde

Cho *et al. Journal of Analytical Science and Technology*   (2022) 13:20

Page 10 of 10

3-phosphate dehydrogenase in human diploid fibroblasts. Exp Mol Med. 2010;42:254–69.

Labat-Robert J. Age-dependent remodeling of connective tissue: role of fibronectin and laminin. Pathol Biol (paris). 2003;51:563–8.

Labat-Robert J, Robert L. Aging of the extracellular matrix and its pathology. Exp Gerontol. 1988;23:5–18.

Lasio MLS, Kozel BA. Elastin-driven genetic diseases. Matrix Biol. 2018;71–72:144–60.

Lee YS, Park CO, Noh JY, Jin S, Lee NR, Noh S, Lee JH, Lee KH. Knockdown of paraoxonase 1 expression influences the ageing of human dermal microvascular endothelial cells. Exp Dermatol. 2012;21:682–7.

Lener T, Moll PR, Rinnerthaler M, Bauer J, Aberger F, Richter K. Expression profiling of aging in the human skin. Exp Gerontol. 2006;41:387–97.

Lettmann S, Bloch W, Maass T, Niehoff A, Schulz JN, Eckes B, Eming SA, Bonaldo P, Paulsson M, Wagener R. Col6a1 null mice as a model to study skin phenotypes in patients with collagen VI related myopathies expression of classical and novel collagen VI variants during wound healing. PLoS ONE. 2014;9:e105686.

Lorenzi M, Lorenzi T, Marzetti E, Landi F, Vetrano DL, Settanni S, Antociocco M, Bonassi S, Valdiglesias V, Bernabei R, Onder G. Association of frailty with the serine protease HtrA1 in older adults. Exp Gerontol. 2016;81:8–12.

Matos L, Gouveia A, Almeida H. Copper ability to induce premature senescence in human fibroblasts. Age (dordr). 2012;34:783–94.

Oender K, Trost A, Lanschuetzer C, Laimer M, Emberger M, Breitenbach M, Richter K, Hitner H, Bauer JW. Cytoskeleton-related loss of cellular integrity is not a major driving force of human intrinsic skin aging. Mech Ageing Dev. 2008;129:563–71.

Oka C, Tsujimoto R, Kajikawa M, Koshiba-Takeuchi K, Ina J, Yano M, Tshuchiya A, Ueda Y, Soma A, Kanda H, Matsumoto M, Katawaichi M. HtrA1 serine protease inhibits signaling mediated by Tgfbeta family proteins. Development. 2004;131:1041–53.

Pflieger D, Chabane S, Gaillard O, Bernard BA, Ducoroy P, Rossier J, Vinh J. Comparative proteomic analysis of extracellular matrix proteins secreted by two types of skin fibroblasts. Proteomics. 2006;6:5868–79.

Rather HA, Mishra S, Su Y, Kumar A, Singh S, Misra BB, Lee J, Furdui CM, Hamilton LR, Gould RW, Nader SH, Nader MA, Deep G. Mass spectrometry-based proteome profiling of extracellular vesicles derived from the cerebrospinal fluid of adult rhesus monkeys exposed to cocaine throughout gestation. Biomolecules. 2022;12:510.

Song H, Zhang L, Luo Y, Zhang S, Li B. Effects of collagen peptides intake on skin ageing and platelet release in chronologically aged mice revealed by cytokine array analysis. J Cell Mol Med. 2018;22:277–88.

Tomela K, Karolak JA, Ginter-Matuszewska B, Kabza M, Gajecka M. Influence of *TGFBR2*, *TGFB3*, *DNMT1*, and *DNMT3A* Knockdowns on CTGF, TGFBR2, and DNMT3A in neonatal and adult human dermal fibroblasts cell lines. Curr Issues Mol Biol. 2021;43:276–85.

Wang D, Kang L, Chen C, Guo J, Du L, Zhou D, Li G, Zhang Y, Mi X, Zhang M, Liu S, Tan X. Loss of legumain induces premature senescence and mediates aging-related renal fibrosis. Aging Cell. 2022;21: e13574.

Wierzbicka-Patynowski I, Mao Y, Schwarzbauer JE. Analysis of fibronectin matrix assembly. Curr Protoc Cell Biol. 2004;Chapter 10, Unit 10.12.

Won CH, Kwon OS, Kang YI, Yoo HG, Lee DH, Chung JH, Kim KH, Park WS, Park NH, Cho K, Kwon SO, Choi J-S, Eun HC. Comparative secretome analysis of human follicular dermal papilla cells and fibroblasts using shotgun proteomics. BMB Rep. 2012;45:253–7.

Yang Z, Camp NJ, Sun H, Tong Z, Gibbs D, Cameron DJ, Chen H, Zhao Y, Pearson E, Li X, Chien J, Dewan A, Harmon J, Bernstein PS, Shcrindhar V, Zabriskie NA, Hoh J, Howes K, Zhang K. A variant of the HTRA1 gene increases susceptibility to age-related macular degeneration. Science. 2006;314:992–3.

Yang KE, Kwon J, Rhim J-H, Choi J-S, Kim SI, Lee S-H, Park J, Jang I-S. Differential expression of extracellular matrix proteins in senescent and young human fibroblasts: a comparative proteomics and microarray study. Mol Cells. 2011;32:99–106.

Yang KE, Jang HJ, Hwang I-H, Hong EM, Lee MG, Lee S, Jang I-S, Choi J-S. Stereoisomer-specific ginsenoside 20(S)-Rg3 reverses replicative senescence of human diploid fibroblasts via Akt-mTOR-Sirtuin signaling. J Ginseng Res. 2020;44:341–9.

Yeo EJ, Hwang YC, Kang CM, Kim IH, Kim DI, Parka JS, Choy HE, Park WY, Park SC. Senescence-like changes induced by hydroxyurea in human diploid fibroblasts. Exp Gerontol. 2000;35:553–71.

Publisher's Note